Hong Kong Baptist University

HKBU Institutional Repository

2012

A random rotor molecule: Vibrational analysis and molecular dynamics simulations

Yu Li
City University of Hong Kong

Rui-Qin Zhang
City University of Hong Kong, aprqz@cityu.edu.hk

Xing-Qiang Shi
Hong Kong Baptist University

Zijing Lin
University of Science and Technology of China, zjlin@ustc.edu.cn

Michel Andre Van Hove
Hong Kong Baptist University, vanhove@hkbu.edu.hk

APA Citation

Li, Y., Zhang, R., Shi, X., Lin, Z., & Van Hove, M. (2012). A random rotor molecule: Vibrational analysis and molecular dynamics simulations. *Journal of Chemical Physics, 137*, 234302-1-234302-6. https://doi.org/10.1063/1.4769779

A random rotor molecule: Vibrational analysis and molecular dynamics simulations

Yu Li, Rui-Qin Zhang, Xing-Qiang Shi, Zijing Lin, and Michel A. Van Hove

Additional information on J. Chem. Phys.

A random rotor molecule: Vibrational analysis and molecular dynamics simulations

Yu Li,[1,2,3] Rui-Qin Zhang,[1,a)] Xing-Qiang Shi,[4] Zijing Lin,[2,a)] and Michel A. Van Hove[4,a)]

[1]*Department of Physics and Materials Science, City University of Hong Kong, Hong Kong SAR, China*
[2]*Department of Physics, University of Science and Technology of China, Hefei, China*
[3]*USTC-CityU Joint Advanced Research Centre, Suzhou, 215123, China*
[4]*Institute of Computational and Theoretical Studies and Department of Physics, Hong Kong Baptist University, Hong Kong SAR, China*

Molecular structures that permit intramolecular rotational motion have the potential to function as molecular rotors. We have employed density functional theory and vibrational frequency analysis to study the characteristic structure and vibrational behavior of the molecule (4′,4′′′′-(bicyclo[2,2,2]octane-1,4-diyldi-4,1-phenylene)-bis-2,2′:6′,2′′-terpyridine. IR active vibrational modes were found that favor intramolecular rotation. To demonstrate the rotor behavior of the isolated single molecule, *ab initio* molecular dynamics simulations at various temperatures were carried out. This molecular rotor is expected to be thermally triggered via excitation of specific vibrational modes, which implies randomness in its direction of rotation. © *2012 American Institute of Physics*. [http://dx.doi.org/10.1063/1.4769779]

In recent years, there has been great interest in molecular machines, in which changes in shape, switching processes, or movements are triggered by external chemical, electrochemical, or photochemical stimuli.[1,2] Many examples of functional molecular devices were reported recently, such as "molecular brakes,"[3] "molecular turnstiles,"[4] "light-switchable catalysts,"[5] "photoresponsive crown ethers,"[6] "photoswitchable fluorophores,"[7] and "chiroptical molecular switches."[8] A most interesting and challenging component of these machines is the molecular rotor, which is commonly defined as a molecular system in which one part (the rotator) rotates relative to the rest (the stator) by a large angle in response to certain stimuli.[9,10] It was recently observed that a rotor molecule named (4′,4′′′′-(bicyclo[2,2,2]octane-1,4-diyldi-4,1-phenylene)-bis-2,2′:6′,2′′-terpyridine[11] (BTP-BCO[12] for short), illustrated in Figure 1(a), could undergo an intramolecular torsional motion around its molecular long axis when approached by a sharp tip and then stimulated by tunneling electrons in a one-electron process occurring in a scanning tunneling microscope. Other molecular motors were reported to be electrically excited,[13] while the widely studied molecular rotor thioether has been demonstrated to be thermally excited.[14] All these rotors share a similar working mechanism in that they are driven by internal vibrational modes excited through electrons, interadsorbate molecular interactions, or molecule-substrate interactions, which in turn are due to an external STM tip.

Most of the investigated rotors mentioned above have a relatively high barrier of rotation in their stable configurations, but start rotating under an external force and are therefore called "driven" rotors. By contrast, "random rotors,"

which have a relatively low barrier of rotation, are easily powered by a thermal source, in which case relatively small amounts of thermal energy can induce rotation of the rotor, while an external field may of course also affect the static configuration of the rotor or cause its unidirectional rotation. The small energy barrier for rotation typical of a "random" rotor favors rotation in the presence of a trigger and, once activated, the rotor may continue rotating without further inducement. Another feature of a "random rotor" is its weak dependence on the environment in that the rotational direction, whether random or unidirectionally favored, is not determined by an external energy source. However, research on "random" rotors is lacking in comparison to "driven" rotors. The working principle of "random" rotors is still under debate, but appears to depend on a subtle equilibrium between the noise spectrum of excitation and the asymmetric potential profile of the moving parts relative to the static ones.[15] As a result, it is of great interest to study molecular structures that permit intramolecular motion and to explore the potential of molecular rotors as molecular machinery. In connection with asymmetric potential profiles, we note here the principle of reciprocity in quantum mechanics, according to which the probability of crossing an asymmetric barrier is nonetheless equal in both directions, i.e., symmetrical (even with a lossy potential).[16]

In this paper, we examine the characteristic structure and vibrational behavior of the abovementioned BTP-BCO molecule[12] via density functional theory (DFT) calculations and demonstrate its rotor behavior via *ab initio* molecular dynamics (MD) simulations. In contrast to the driven rotors with external stimuli such as light or an STM tip, this isolated rotor molecule presents rotor behavior at suitable temperatures and manifests spontaneous rotation due to asymmetric vibrational excitation.

The geometric structures, vibrational infrared, and resonant Raman spectra of the molecular rotor were

---

a)Authors to whom correspondence should be addressed. Electronic addresses: aprqz@cityu.edu.hk, zjlin@ustc.edu.cn, and vanhove@hkbu.edu.hk.

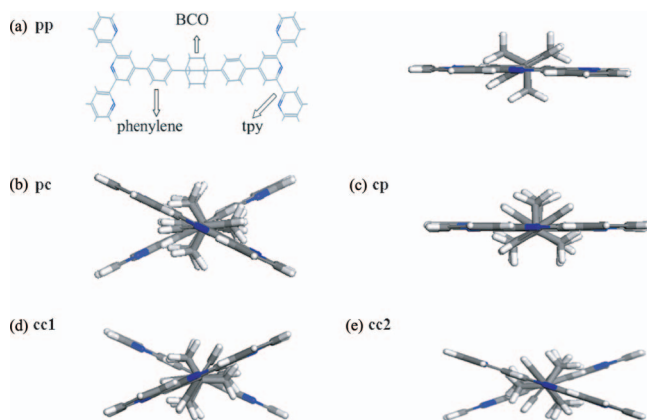**137**, 234302-1 © 2012 American Institute of Physics

FIG. 1. Top and side views of the pp structure (a) and side views (b)-(e) of the other isomer structures of the rotor molecule BTP-BCO. Three molecular groups are labeled in (a). (The detailed structural information and the naming method is in the supplementary material[25]).

systematically studied using density functional theory (DFT), with the Becke three-parameter Lee-Yang-Parr (B3LYP) exchange-correlation functional, which combines the Becke three-parameter hybrid functional with the gradient-corrected correlation functional of Lee-Yang-Parr,[17, 18] as implemented in the GAUSSIAN 03 code.[19] A composite basis set was used, namely 6-31G#,[20] where a 6-31G* basis set was added for the negatively charged nitrogen atoms, while 6-31G was added for the positively charged carbon and hydrogen atoms. After optimization, a higher standard basis set 6-31G* was applied for a single point energy calculation of the geometries obtained upon the composite basis. Normal modes of vibration are calculated within the harmonic approximation from a force constant matrix.

We performed *ab initio* MD simulations using the Nose algorithm within the Perdew-Burke-Ernzerhof (PBE) form of the generalized gradient approximation (GGA) xc-potential[21] implemented in the SIESTA 3.0 code.[22] The pseudopotentials were constructed using the Trouiller and Martins scheme.[23] A split-valence double-ζ basis set with polarization orbitals (DZP) was set for all the atoms. Charge density was presented on a real space grid mesh equivalent of a plane-wave cutoff of 200 Ry. A cubic supercell, with dimensions 40 Å × 40 Å × 40 Å, was built with an inside vacuum space large enough to treat the rotor molecule as isolated. Only the Gamma point in k-space was calculated and the orbital energy shift, which defines the confinement radii of different orbitals, was 100 meV. The simulations were performed under the conditions of constant temperature and constant volume (NVT) ensemble. A time step of 1 fs was used to integrate Newton's equation of motion.

Figure 1(a) shows the chemical structure of the rotor molecule BTP-BCO. It consists of two terminal terpyridine (tpy) groups, a central bicyclo[2,2,2]octane (BCO) group acting as the rotator and two phenylene groups. The BCO group has three-fold axial symmetry, with three C-C-C-C chains. We designed and then optimized five initial geometries by combining independently optimized conformations of sectional groups (see the supplementary material[25] for details). The fully optimized geometries differ by quite small energies

(Figure S4 in the supplementary material[25]). The five groups within the molecule (BCO, two phenylenes and two tpys) are almost rigid, so the molecule only has four significant degrees of internal rotational freedom: the four dihedral angles between adjacent groups (Table S1 and Figure S2 in the supplementary material[25]). Intramolecular rotation can be thought of as a process of isomerization between these conformations (the side views are shown in Figures 1(a)–1(e). To prove this assumption and gain deeper insight into the intramolecular motion of the molecule, we performed vibrational spectrum analyses and molecular dynamics simulations of the representative pp geometry (Figures 1(a) and 2(b), also see the pp geometry in Figure S2a in the supplementary material[25]). To confirm the generalization of the result, similar calculations were also performed for the cp geometry (Figure 1(c), also see Figure S6 in the supplementary material[25]).

The IR spectrum of the molecule (in the pp geometry) is shown in Figure 2(a). The vibrational modes of the five molecular groups are coupled and combined, and hence a comprehensive analysis of the vibrational modes would be complex, while it is also not our central purpose. We checked all the vibrational modes individually by visualization of the actual motion of the rotor molecule. We observe that at certain frequencies, such as 851 cm^{-1}, where the infrared intensity is 2.86 KM/Mole, the corresponding wagging vibration of the C-H bonds of the BCO group and the phenylene group may favor the rotation of this part (shown by arrows in Figure 2(b)). Similar modes also exist between 770 cm^{-1} and 1000 cm^{-1}, for example, at 842 cm^{-1} and 867 cm^{-1}. Such vibration modes favoring the rotation of the BCO part also exist in the cp structure (see Figure S6 in the supplementary material[25]). The infrared intensity at 867 cm^{-1} is as high as 35.4 KM/Mole. A useful feature is that these vibrational modes with intramolecular rotational character are IR active (as shown with an arrow in Figure 2(a)) but not Raman active. To date, no experimental data or theoretical calculations for the IR and Raman spectra (Figure S5b in the supplementary material[25]) of this wheel molecule were available, so our results will be useful for future research on related issues.

We estimate the rotational barrier of this molecule to be ~170–190 meV by the following method: the total energies of the geometries with the BCO group rotated from the pp geometry are calculated every 15° to describe the rotational potential surface; for the representative geometries rotated by 60°, –60°, 120°, and –120° from the initial pp geometry, overall optimizations are performed; for the other involved geometries, the total energy is calculated by single point energy calculation (optimizations always lead to the pp geometry), see Figure 2(c). The calculated rotational barrier here is overestimated since the calculated geometries are not all local minima or transition states. The calculated rotational barrier here is overestimated in part because the geometry of the transition state cannot be determined exactly, but more importantly because we do not in this "static" estimate include vibrations or rotations; in the latter case thermal energy can, temporarily and by coincidence, provide additional kinetic energy to overcome the barrier, for example; this effectively reduces the "dynamic" barrier height, as we will see below with molecular dynamics. Therefore, the actual torsional
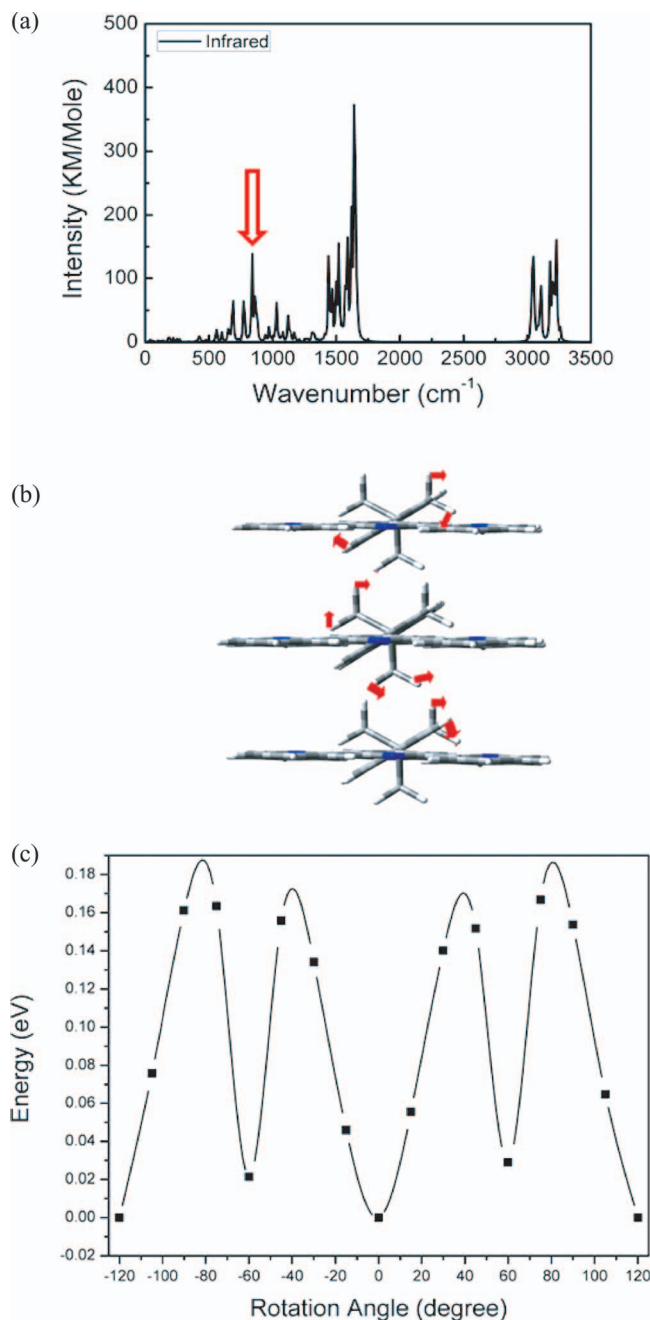
(a)

(b)

(c)

FIG. 2. (a) Calculated IR spectrum of the parallel-parallel (pp) geometry of the rotor molecule shown in (b). The red arrows in (b) indicate important vibrational displacements for three vibrational modes, at 851 cm^{-1} (at top), 842 cm^{-1} (at center), and 867 cm^{-1} (at bottom), seen along the long axis of the molecule. (c) shows the rotational barriers of this wheel molecule in two opposite directions: clockwise (positive angles) and anticlockwise (negative angles), starting from 0° for the pp structure shown in (b).

FIG. 3. Snapshots of MD simulations of the parallel-parallel (pp) geometry at 450 K, at times t = 0 ps (a), 0.7 ps (b), 1.6 ps (c), and 2.5 ps (d). The direction of view is constant, perpendicular to the initial molecular plane in (a). A carbon atom is colored red to highlight the rotation of the central BCO group.

support the rigid model of the wheel molecule, which will be discussed further below.

The specific conformations, the small rotational barrier of the molecule and the relevant vibrational modes all indicate a molecular rotor. While a static exploration of the geometry and vibrations provides only an incomplete study of rotor behavior, molecular dynamics (MD) simulation is available for an understanding and confirmation of rotor motion. MD simulations at different temperatures ranging from 100 K to 450 K were thus carried out with one of the five optimized conformations (the pp geometry, shown in Figures 1(a) and S2 in the supplementary material[25]) of the molecule as the initial structure. With rising temperature the central BCO group generally underwent an increasingly long unidirectional rotation around the molecular long axis before stopping and turning back, while the other groups manifested more random thermal motion. Snapshots of one MD simulation at 450 K are shown in Figure 3 with one carbon atom in the rotor colored differently to clearly exhibit the rotation. From the initial structure (Figure 3(a)), the BCO group has rotated by 120° in ∼0.7 ps (Figure 3(b)), while the rest of the molecule shows indistinct rotation. While the BCO group has turned significantly further after ∼1.6 ps (Figure 3(c)), the tpy groups exhibit notable torsion and a non-planar geometry. In Figure 3(d), the colored carbon atom has almost returned to its initial position, having achieved a full rotational cycle, while the rest of the molecule has rotated less than 90°. Multiple independent MD runs show similar rotation behavior but the specific rotational direction depends on the (random) distribution of the initial velocities.

To present a detailed view of intramolecular rotation of the rotor molecule, we show in Figure 4 snapshots of the first 120° jump of the BCO group at 400 K. The snapshots are drawn for the local minima of the total-energy curve (shown in Figure 5), which correspond to typical conformations of interest. The initial geometry is shown in Figure 4(a), with one carbon-carbon (C-C) bond of the rotor highlighted in yellow. After 74 fs, as shown in Figure 4(b), this C-C bond exhibits notable twisting torsion due to asynchronous rotation around the long molecular axis, relative to the slower remaining parts of the molecule. The phenylene rings initially show asymmetric motion, the left one rotating while the right one remains almost static. The rotation of the BCO rotor and the phenylene ring can be ascribed to the above mentioned

barrier should be smaller, which favors rotation activated by thermal energies. The rotational barrier presents a nearly symmetric character, when comparing the two peaks on either side of the initial structure (pp), corresponding to 0° rotation in Figure 2(c). That is, the pp structure is expected to rotate in either direction with nearly equal probability. Since the pp structure is actually asymmetrical, it is noted that rotation in opposite directions generates nonequivalent structures. Thus, the nearly symmetric rotational barriers for the pp structure
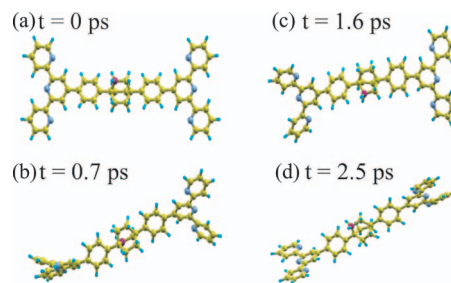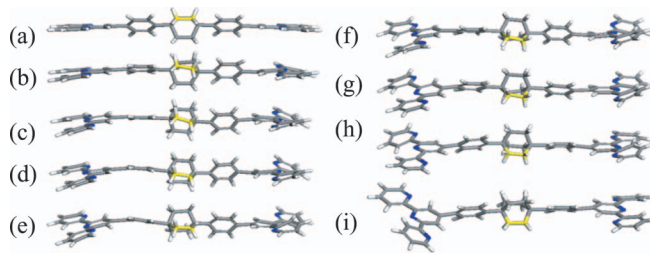
FIG. 4. Snapshots of MD simulations of the parallel-parallel geometry at 400 K (with a constant direction of view). (a) at time t = 0 fs, (b) t = 74 fs, (c) t = 171 fs, (d) t = 237 fs, (e) t = 294 fs, (f) t = 349 fs, (g) t = 422 fs, (h) t = 497 fs, (i) t = 745 fs. One of the rotor's carbon-carbon bonds is colored yellow as reference for the rotation.

FIG. 6. Maximum rotational angle θ and "time to stop" t until first reversal of rotation, as a function of temperature, from individual MD simulations. The calculated MD data points are connected by lines to guide the eye.

vibration modes shown in Figure 2(a). We also observe that this kind of asymmetric motion of the phenylene rings may lead to transformation between the molecule isomers, since the dihedral angle between two phenylene rings is one important factor. For example, the structure of Figure 4(d) was optimized to be an isomer of the initial structure among the aforementioned five optimized conformations (as shown in Figure 1(c) and Figure S2c). In Figs. 4(c) and 4(f), the C-C bond has rotated by about 30° and 60°, respectively, from its initial orientation. After 496 fs, as shown in Figure 4(h), the C-C bond has undergone a further 30° jump and reaches about 90° in total. Finally, in Figure 4(i), the C-C bond has completed its first 120° jump. As shown in Figure 5, the molecules in Figures 4(c), 4(f), 4(h), and 4(i) correspond to some of the local minima in the total energy. The thermal energy corresponding to 400 K is ∼0.12 eV (estimated as $\frac{1}{2}$ fk_BT,[24] with f chosen as 7 for larger molecules). This is comparable to the overestimated rotational barrier of rotation visible in Figure 2(c) whose profiles are nearly symmetrical when comparing clockwise and anticlockwise rotations. This coincidence also explains the onset of a full rotation of 360° at 400 K. We see that the rotation proceeds at a relatively constant speed since the rotation angle θ is approximately proportional
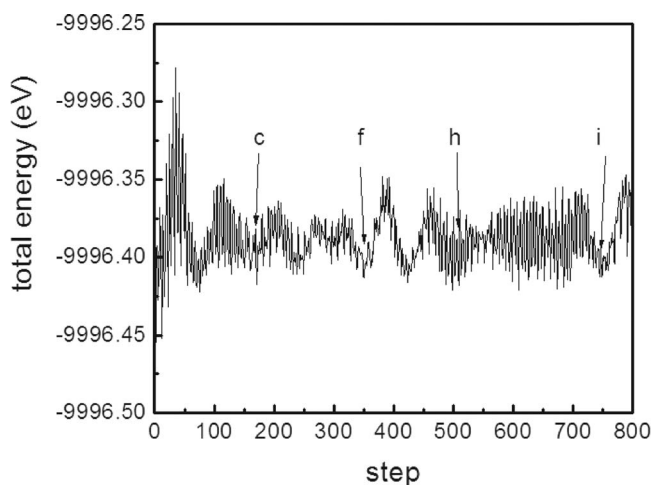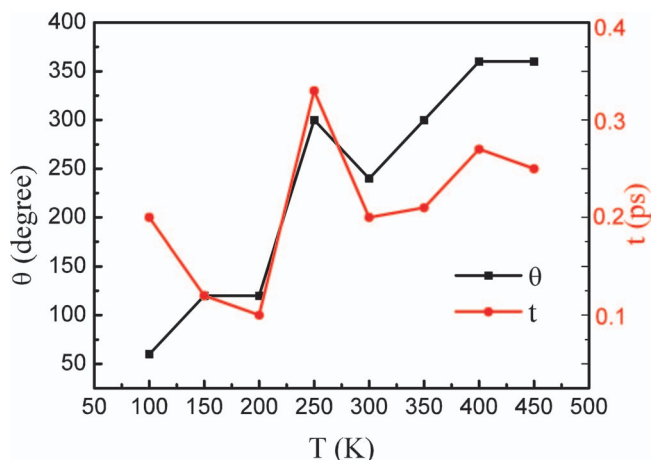

FIG. 5. Total energy vs step from MD simulation at 400 K, (each time step is 1 fs). The arrows denoted as c, f, h, and i show four local energy minima where snapshots of the molecule are extracted for Fig. 4(c), f, h, and i, respectively. At these four points, the BCO group has undergone rotation by 30°, 60°, 90°, and 120°, respectively.

to time, as shown in Figure 6 for a full turn; this further confirms that the rotational barrier is low, estimated to be rather less than 0.2 eV, since a higher barrier would make the rotation slow down considerably near the top of the barrier, i.e., near position f in Figure 5.

The "performance" of the rotor can be judged by: (1) the maximum rotational angle θ reached before the rotation stops and turns back; and (2) the "time to stop" t needed to reach that maximum rotational angle. Figure 6 shows that these two performance criteria clearly fluctuate in different MD trajectories, due to the different random initial velocities of the atoms in the molecule. Since a systematic study of these multiple and complex processes would require a prohibitively large number of MD runs to become statistically significant, our analysis instead will focus on the qualitative behavior of the rotation as exhibited by one arbitrarily selected MD trajectory at each temperature. From these MD runs, we see in Figure 6 that, as temperature increases, the rotor tends to rotate farther (larger maximum rotational angle θ), roughly proportionally to temperature; this maximum angle also takes longer to reach (larger time to stop t), but this duration seems to grow more slowly with temperature (clearly, sharp statistical deviations occurred at 100 K and 250 K). One can expect this trend: at higher temperatures, more energy is available to keep the rotor turning by inertia before rotational kinetic energy is fed back into vibrational modes, in rough proportion to the available energy. On the other hand, the duration of that rotation must be related to the (angular) speed, which grows more slowly with increasing temperature, namely about proportionally to the square root of the kinetic energy or temperature, as observed very qualitatively in Figure 6.

It is helpful to consider such MD runs in terms of more elementary collective motions. For the molecule as a whole, a random initial MD configuration gives it in general a net nonzero linear momentum, i.e., its center of mass will move with a constant velocity vector due to conservation of linear momentum (regardless of internal motions, except for numerical artifacts of the MD simulation). Similarly, the molecule as a whole will in general rotate around a certain axis with a net

non-zero constant angular velocity due to conservation of angular momentum. Each internal normal mode of vibration will also remain constant (in amplitude and phase), since these normal modes are in principle decoupled from each other.

More interesting are internal motions of the five constituent groups of the molecule, in particular the BCO rotor. Each group will initially also have its individual net linear and angular momenta due to the random initial configuration; for example, the central rotor as a whole may start with some random velocity vector and some random angular momentum component around its main axis. But the linear and angular motions of the five different groups are coupled together and thus can exchange energy over time; the central rotor in particular can change its rotation speed, and reverse its direction of rotation. In addition, the internal modes of vibration of the individual molecular groups are now also coupled to the linear, rotational, and vibrational motions of the neighboring groups. Therefore, continuous exchanges of energy will occur among all these collective modes of motion. Our MD simulations exhibit all these behaviors, as illustrated in particular in Figure 4.

We can now interpret in more detail the thermal behavior of this single molecular rotor by analyzing the interplay between two important quantities: the magnitude of the rotational potential and the thermal energy. The former reflects the energetic barrier described by the potential energy surface and the latter contributes to the thermal vibrations. For this random hindered rotor, thermally activated hopping over the potential barrier is the main method of rotator reorientation. At low temperatures, thermally activated hops are rare and small, so the rotor rarely reorients. This corresponds to smaller θ, and therefore also smaller t, as exhibited qualitatively in Figure 6 (again we consider the "spikes" at 100 and 250 K to be statistical fluctuations). As the temperature increases, thermally activated hops become more common, resulting in enhanced θ. In this case, θ grows and so does t, as we see in Figure 6.

The profile of the rotational potential and the thermal energy implies a random rotational direction of this molecule. While our MD simulations exhibit 100% clockwise rotation, this may be ascribed to the statistically small number of our MD runs (4 runs for the pp structure at 400 K). Thus, a larger number of MD runs are expected to remove this apparently favored unidirectional rotation. The (random) distribution of the initial velocities and energies assigned in MD is another variable in determining the initial rotational direction. It should be noted that such unidirectional motion can only exist within a limited time scale since the vibrational modes and the rotational barrier vary with the instantaneous structure in addition to the exchange of energy and angular momentum between the rotor and other parts of the molecule. Overall, the wheel molecule should rotate in a random direction. As presented in the MD trajectory, the molecule will certainly stop its rotational motion; it can then start rotating again, either in the same or in the opposite direction; nonetheless, our simulations illustrate very clearly that the rotor can rotate relatively far, once it is in unidirectional motion.

In conclusion, the thermally activated hops are achieved by thermally activating vibrational modes that involve rota-

tional motion of the rotor. As shown in the section describing the vibrational frequency analysis, the rotor has many degrees of freedom, among which exists the ability to turn through a single torsional angle. However, the other molecular degrees of freedom due to thermal motion of atoms within the rotor comprise part of the thermal bath with which the single torsional degree of freedom interacts. The torsional and non-torsional modes in a rotor system are inherently coupled, although the extent of the coupling will depend on the rotor structure. In layman's terms, biological machines maintain operation within an environment where fluctuations and vibrations exceed the actual motions of the machines and they may actually use or rectify such fluctuations as an operational principle. Here, we attribute the rotation of the rotor to favorable thermal fluctuations. The collaboration of the series of vibrational modes as well as certain rotational modes contributes to the intramolecular motion at temperatures such that the thermal fluctuations excite the vibrations and exceed the energetic barrier of the rotation.

For TP-BCO, we predict a rotor behavior based on specific structural and vibrational analysis and present MD simulations to demonstrate its intramolecular rotation at various temperatures. The particular vibrational modes excited due to a favorable thermal fluctuation break the near-symmetry of the potential and favor directional torsion once excited, even though the thermal environment has no directional preference. This spontaneous uniaxial rotation makes the rotor uniquely interesting in that it requires little human control of the external environment of the rotor group and is more available for stimulation.

[1]K. Mislow, Chemtracts-Org. Chem. **2**, 151–174 (1989); M. Irie, Chem. Rev. **100**, 1683–1716 (2000); V. Balzani, M. Gómez-López, and J. F. Stoddart, "Molecular machines," Acc. Chem. Res. **31**, 405–414 (1998); J.-P. Sauvage, Acc. Chem. Res. **31**, 611–619 (1998); V. Balzani, A. Credi, F. M. Raymo, and J. F. Stoddart, Angew. Chem., Int. Ed. **39**, 3348–3391 (2000).

[2]B. L. Feringa, W. F. Jager, and B. de Lange, Tetrahedron **49**, 8267–8310 (1993).

[3]T. R. Kelly, M. C. Bowyer, K. V. Bhaskar, D. Bebbington, A. Garcia, F. Lang, M. H. Kim, and M. P. Jette, J. Am. Chem. Soc. **116**, 3657–3658 (1994).

[4]T. C. Bedard and J. S. Moore, J. Am. Chem. Soc. **117**, 10662–10671 (1995).

[5]F. Würthner and J. Rebek, Jr., Angew. Chem., Int. Ed. Engl. **34**, 446–448 (1995).

[6]S. Shinkai, T. Ogawa, Y. Kusano, O. Manabe, K. Kikukawa, T. Goto, and T. J. Matsuda, Am. Chem. Soc. **104**, 1960–1967 (1982).

[7]G. M. Tsivgoulis and J.-M. Lehn, Angew. Chem., Int. Ed. **34**, 1119–1122 (1995).

[8] B. L. Feringa, W. F. Jager, B. de Lange, and E. W. Meijer, J. Am. Chem. Soc. **113**, 5468–5470 (1991); W. F. Jager, J. C. de Jong, B. de Lange, N. P. M. Huck, A. Meetsma, and B. L. Feringa, Angew. Chem., Int. Ed. **34**, 348–350 (1995); B. L. Feringa, N. P. M. Huck, and H. A. van Doren, J. Am. Chem. Soc. **117**, 9929–9930 (1995).

[9] E. R. Kay, D. A. Leigh, and F. Zerbetto, Angew. Chem. **119**, 72–196 (2007); Angew. Chem., Int. Ed. **46**, 72–191 (2007).

[10] V. Balzani, A. Credi, and M. Venturi, *Molecular Devices and Machines: A Journey into the Nano World* (Wiley VCH, Weinheim, 2003).

[11] F. Barigelletti, L. Flamigni, V. Balzani, J.-P. Collin, J.-P. Sauvage, and A. Sour, New. J. Chem. **19**, 793–798 (1995).

[12] W. H. Wang, X. Q. Shi, M. Jin, C. Minot, M. A. Van Hove, J.-P. Collin, and N. Lin, ACS Nano **4**, 4929–4935 (2010).

[13] H. L. Tierney, C. J. Murphy, A. D. Jewell, A. E. Baber, E. V. Iski, H. Y. Khodaverdian, A. F. McGuire, N. Klebanov, and E. C. H. Sykes, Nat. Nanotechnol. **6**, 625–629 (2011); T. Kudernac, N. Ruangsupapichat, M. Parschau, B. Maciá, N. Katsonis, S. R. Harutyunyan, K. H. Ernst, and B. L. Feringa, Nature (London) **479**, 208–211 (2011); H. W. Kim, M. Han, H.-J. Shin, Y. Oh, K. Tamada, M. Hara, Y. Kim, M. Kawai, and Y. Kuk, Phys. Rev. Lett. **106**, 146101 (2011).

[14] A. E. Baber, H. L. Tierney, and E. C. H. Sykes, ACS Nano **2**, 2385–2391 (2008).

[15] R. D. Astumian, Science **276**, 917–922 (1997).

[16] D. E. Bilhorn, L. L. Foldy, R. M. Thaler, W. Tobocman, and V. A. Madsen, J. Math. Phys. **5**, 435 (1964).

[17] C. Lee, W. Yang, and R. G. Parr, Phys. Rev. B **37**, 785–789 (1988).

[18] A. D. Becke, J. Chem. Phys. **98**, 5648–5652 (1993).

[19] M. J. Frisch, G. W. Trucks, H. B. Schlegel *et al.*, GAUSSIAN 03, Revision C.02 (Gaussian, Inc., Wallingford, CT, 2004).

[20] R. Q. Zhang, N. B. Wong, S. T. Lee, R. S. Zhu, and K. L. Han, Chem. Phys. Lett. **319**, 213–219 (2000).

[21] J. P. Perdew, K. Burke, and M. Ernzerhof, Phys. Rev. Lett. **77**, 3865 (1996); **78**, 1396 (1997).

[22] P. Ordejon, E. Artacho, and J. M. Soler, Phys. Rev. B **53**, 10441–10444 (1996); J. M. Soler, E. Artach, J. D. Gale, A. Garcia, J. Junquera, P. Ordejon, and D. Sanchez-Portal, J. Phys.: Condens. Matter. **14**, 2745–2779 (2002).

[23] N. Troullier and J. L. Martins, Phys. Rev. B **43**, 1993 (1991).

[24] D. V. Schroeder, *An Introduction to Thermal Physics* (Addison-Wesley, 1999), p. 15.

[25] See supplementary material at http://dx.doi.org/10.1063/1.4769779 for a random rotor molecule: Vibrational analysis and molecular dynamics simulations.